

# AN INVESTIGATION OF PERIODIC ROD STRUCTURES FOR YAGI AERIALS

By J. O. SPECTOR, Ph.D., Associate Member.

(*The paper was first received 17th May, and in revised form 9th August, 1957.*)

## SUMMARY

The periodic structure of conducting rods, normally used for Yagi-type aerials, is investigated from the point of view of a guide for surface waves. In a series of resonator experiments it is found that a non-radiating plane surface wave of the HE<sub>11</sub>-mode may be guided along the structure, and that radiation occurs only from a discontinuity. The guiding effect is found to exist only where the rod lengths are less than  $\lambda/2$ . The structure is thus analogous to a capacitively-loaded transmission line. The propagation coefficients are experimentally determined for structures of different rod length and spacing. These propagation coefficients are used to predict the radiation patterns of Yagi aerials in conjunction with the theory outlined in a previous paper. There is quite good agreement with experimentally-observed radiation patterns of long Yagi aerials. The side-lobe structure is explained by interference with direct radiation from the driven element caused by inefficient launching of the surface wave.

## LIST OF PRINCIPAL SYMBOLS

- $\lambda_0$  = Free-space wavelength of frequency  $f_0$ .
- $\lambda_g$  = Guided wavelength on guiding structure.
- $\rho, \phi$  = Cylindrical co-ordinates.
- $\theta$  = Angle with aerial axis.
- $g(\theta)$  = Amplitude radiation pattern.
- $F(\rho, \phi)$  = Amplitude distribution in aperture plane.
- $\beta, \beta_0$  = Phase-change coefficients of guided wave and free-space wave, respectively.
- $Z_0, Z_1$  = Characteristic wave impedances of unloaded and loaded transmission line, respectively.
- $d$  = Spacing of periodic elements.
- $h$  = Length of copper rods.
- $\epsilon_r$  = Relative permittivity of supporting dielectric rod.
- $v_1, v_0$  = Phase velocities of surface wave on periodic structure and free-space wave, respectively.
- $\delta f$  = Shift of resonance frequency of surface-wave resonator.
- $f_0$  = Initial resonance frequency of surface-wave resonator, with  $l = 0$ .
- $L$  = Length of surface-wave resonator.
- $l$  = Length of loaded section.
- $K$  = Constant defined by eqn. (13).
- $k_0 = \sqrt{(\beta^2 - \beta_0^2)}$ .
- $A$  = Arbitrary constant.
- $E_x, E_y$  = Components of electric field.
- $J_n(x), K_n(x)$  = Bessel functions.
- $t = Z_1/Z_0$ .
- $u = \frac{\beta_0}{2} \sin \theta$ .

## (1) INTRODUCTION

The common Yagi aerial, as shown in Fig. 1, consists of one driven element and one or more passive, or parasitic, elements. The analysis of this structure is usually made by assuming that

Written contributions on papers published without being read at meetings are invited for consideration with a view to publication.

Dr. Spector was formerly in the Electrical Engineering Department, Imperial College of Science and Technology, London University, and is now at the Ministry of Defence, Israel.

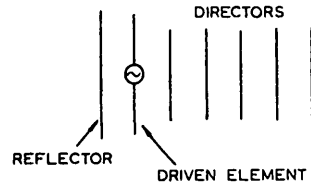


Fig. 1.—Yagi aerial.

the driven element induces currents in the other elements, and in consequence they become radiators themselves. If these induced currents are calculated, the radiation pattern of the aerial will be given by the superposition of the individual radiation fields contributed by each element. To calculate the currents, the structure is considered equivalent to a linear network,<sup>1</sup> and the voltage and current relations are given by

$$[Z_{nm}] [I_n] = [V_n] \quad \dots \quad (1)$$

where  $V_n$  and  $I_n$  are voltages and currents in the element  $n$  of the structure and  $Z_{nm}$  is the mutual impedance (or self-impedance in the case  $n = m$ ) of the elements denoted by the subscripts. In the case of the Yagi aerial, where only one element  $p$  is driven,  $V_n$  in eqn. (1) is made zero except when  $n = p$ .

When eqn. (1) is applied in practice, it is immediately observed that the calculation of the coefficients  $Z$  is extremely difficult, as there are  $n(n + 1)/2$  such coefficients for an  $n$ -element aerial. Indeed, this approach has not yielded useful results for structures of more than a few elements.

A new approach to the problem has been suggested.<sup>2</sup> The periodic structure of conducting elements is considered as an artificial dielectric, along which a surface wave<sup>3,4</sup> is propagated. No radiation takes place from points along the length of the structure. There is, however, radiation from the discontinuity at the end of the structure, and the mechanism of radiation can be described in a very similar way to that of the dielectric rod, and other end-fire structures.

A complete theoretical analysis of the Yagi-type structure in terms of a non-radiating plane surface wave would require the knowledge of the field configuration in the vicinity of the structure. By formulating continuity conditions for the fields at the boundary of the structure the propagation coefficient could be calculated, following the analysis given by Stratton<sup>5</sup> for plane waves on cylindrical guides. The radiation pattern may now be calculated by assuming the transverse components of the field outside the structure to be identical to those of a plane surface wave of the 'dipole mode' type. The radiation pattern of a transverse field distribution  $F(\rho, \phi)$  in the aperture plane is given by<sup>6</sup>

$$g(\theta, X) = (1 + \cos \theta) \int_0^\infty \int_0^{2\pi} F(\rho, \phi) \exp [j\beta_0 \rho \sin \theta \cos(X - \phi)] \rho d\rho d\phi \quad (2)$$

where  $g(\theta, X)$  is the field intensity at a point on the surface of a sphere specified by the polar angles  $\theta$  and  $X$ . However, the field

configuration near the structure is unknown. It is therefore proposed to find the propagation coefficient experimentally, and, assuming that any distortion of the field near the structure decreases very rapidly in the radial direction, to find the radiation pattern by using the field distribution of a pure dipole-mode wave in conjunction with the aperture field method given in eqn. (2).

The purpose of the experimental investigation of the problem was to find whether the periodic structure shown in Fig. 2 could

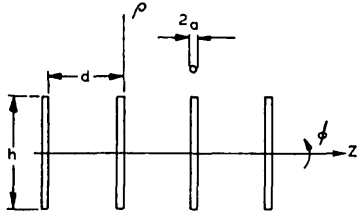


Fig. 2.—Periodic structure of conducting rods.

provide a guiding effect which is required for the propagation of a non-radiating surface wave along itself, and, once the existence of such a guiding effect is established, to find the propagation coefficient as a function of the structural dimensions. Finally, it was proposed to find whether, using these experimental results, a quantitative as well as qualitative description of the Yagi aerial could be given, which would be consistent with measured radiation patterns of Yagi aerials.

#### (2) ANALOGY WITH LOADED TRANSMISSION LINE

Some results of a qualitative nature can be found by using the transmission-line analogy for any particular mode of propagation. The hypothetical transmission of a homogenous plane wave in the absence of the structure of conducting rods can be represented by a transmission line of characteristic impedance  $Z_0$  and phase-change coefficient  $\beta_0 = 2\pi/\lambda_0$ . The addition of conducting rods periodically along the line of propagation may be represented in this transmission-line analogy by impedances shunted across the line at regular intervals. The analysis of the periodically-loaded transmission line shown in Fig. 3 presents no

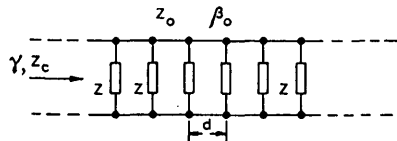


Fig. 3.—Loaded transmission line.

$Z_0$  and  $\beta_0$  are the characteristic impedance and phase-change coefficient, respectively, of the unloaded line.

difficulties, and the propagation coefficient  $\gamma = \alpha + j\beta$  of the loaded line is given by<sup>6</sup>

$$\cosh \gamma d = \cos \frac{2\pi}{\lambda_0} d + \frac{jZ_0}{2Z} \sin \frac{2\pi}{\lambda_0} d \quad \dots \quad (3)$$

where  $Z$  is the impedance of the load.

If it is assumed that there is no radiation from elements along the structure, and if losses in the elements themselves are neglected, the shunt impedance becomes a pure reactance  $Z = jX$  and the line will propagate unattenuated waves ( $\gamma = j\beta$ ) whenever

$$\left| \cos \frac{2\pi}{\lambda_0} d + \frac{Z_0}{2X} \sin \frac{2\pi}{\lambda_0} d \right| \leq 1 \quad \dots \quad (4)$$

The guided wavelength  $\lambda_g$  will be given by

$$\cos \frac{2\pi}{\lambda_g} d = \cos \frac{2\pi}{\lambda_0} d + \frac{Z_0}{2X} \sin \frac{2\pi}{\lambda_0} d \quad \dots \quad (5)$$

It can be seen from eqn. (5) that the guided wavelength is a function of the shunt impedance and the spacing  $d$ .

For small spacings ( $d/\lambda \ll 1$ ) and large shunt impedances, eqn. (5) can be rewritten

$$-\left(\frac{2\pi d}{\lambda_g}\right)^2 \approx -\left(\frac{2\pi d}{\lambda_0}\right)^2 + \frac{Z_0}{2X} \frac{2\pi d}{\lambda_0} \quad \dots \quad (6)$$

which means that  $X$  must be negative in order to reduce the phase velocity ( $\lambda_g < \lambda_0$ ), thus making the wave physically feasible. Hence it can be deduced from the transmission-line analogy that capacitive loading is required. This suggests that the shunt element may be realized in practice by a cylindrical conductor of less than the half-wave resonant length.

#### (3) GENERAL DESCRIPTION OF MEASURING TECHNIQUE AND APPARATUS

A general block schematic of the equipment used for the experiments is given in Fig. 4. The periodic structure was mounted in a surface-wave resonator,<sup>7</sup> which consisted of two

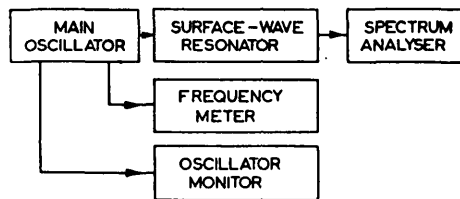


Fig. 4.—Block schematic of apparatus.

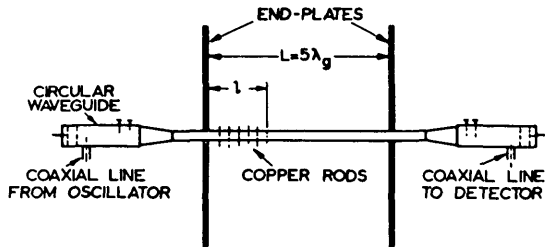


Fig. 5.—Surface-wave resonator.

aluminium plates parallel to one another and at right-angles to the axis of the structure, as shown in Fig. 5. The dimensions of the end-plates were 60 cm × 60 cm, which were large enough to contain almost all the energy of the surface-wave fields inside the resonator, for a wavelength of 10 cm used throughout the experiments. Energy was fed into the resonator through circular holes of 5 cm diameter cut in the centre of each resonator plate. The copper conductors were embedded in cylindrical holes drilled in a polystyrene rod of circular cross-section. The dielectric rod provided some initial guidance for waves along its surface. A rod of 2.54 cm diameter was used, along which the phase velocity of the HE<sub>11</sub>-wave was reduced by  $2 \times 10^{-3}$  of its free-space value.<sup>8</sup>

The HE<sub>11</sub> surface wave on the dielectric rod was launched by means of a circular dielectric-filled waveguide in which the dominant H<sub>11</sub>-mode had been excited. The dielectric was constructed so as to continue from the end of the waveguide and

## SPECTOR: AN INVESTIGATION OF PERIODIC ROD STRUCTURES FOR YAGI AERIALS

was gradually reduced to the dielectric-rod diameter by means of a taper section. Power was fed into the waveguide by means of coaxial cable and probe from a type CV238 reflex klystron.

The output section was identical to the input section. High-frequency power was transmitted by coaxial cable to a spectrum analyser, where it was rectified and presented on a cathode-ray tube in the form of a vertical deflection whose height varied according to the power input.

The frequency of oscillation was accurately measured by a heterodyne crystal-calibrated frequency meter. A small amount of power was extracted for this purpose directly from the oscillator cavity by coaxial cable.

In the absence of any copper rods, the end-plates were adjusted in such a position that a resonance could be observed on the cathode-ray tube for a frequency within the range of the oscillator valve. At the resonance frequency of the system, maximum power was obtained at the spectrum-analyser input terminals, and thus a maximum deflection on the cathode-ray-tube screen was observed. The resonance frequency was found by tuning simultaneously the cavities of the main oscillator valve and the beat-frequency oscillator of the spectrum analyser, while observing the height of the deflection on the cathode-ray tube. At the same time care was taken to operate both klystrons at the centre of their modes of oscillation, so as to avoid spurious amplitude changes, by adjusting the reflector voltages. When a resonance had been established the tuning of the beat-frequency oscillator cavity was left unchanged and its frequency-modulating voltage reduced, thus producing a large shift of the deflection along the time-base of the cathode-ray tube for a small change in main oscillator frequency. The resonance point could be located accurately on the screen, and the frequency of resonance measured by means of the frequency meter.

The system of guiding structure and end-plates is analogous to a transmission line short-circuited at both ends, for any one mode of propagation in the structure. The condition for resonance, or natural oscillations, on such a line is that the sum of impedances 'seen' from any cross-section of the line is equal to zero.<sup>9</sup> The resonator partly filled to a length  $l$  with conducting rods is therefore equivalent to the section of transmission line shown in Fig. 6, where  $v_0$  is the phase velocity along

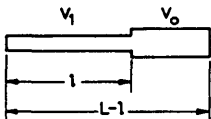


Fig. 6.—Transmission line short-circuited at both ends.

the dielectric rod and  $v_1$  is the phase velocity along the periodic structure of length  $l$ . Taking the cross-section at the discontinuity of the line, the conditions for resonance are\*

$$\tan \frac{\omega}{v_0} (L - l) + \tan \frac{\omega}{v_1} l = 0 \quad . . . \quad (7)$$

When no copper rods are present ( $l = 0$ ), the frequency is denoted by  $\omega_0$ , and the condition for resonance is

$$\begin{aligned} \frac{\omega_0}{v_0} L &= n\pi \\ \text{or } L &= n \frac{\lambda_0}{2} \end{aligned} \quad . . . \quad (8)$$

where  $n$  is an integer and  $\omega_0/v_0 = 2\pi/\lambda_0$ . This means that, at resonance, the length of the resonator must be equal to an

\* In eqn. (7) it is assumed that the line is loss-free and that the two parts of the line have the same characteristic impedance. The effect of a change in characteristic impedance is treated in Section 8.

integral number of half-wavelengths in the resonator. When conducting rods are inserted, the resonance frequency is  $\omega = \omega_0 + \delta\omega$ . From eqn. (7) we have, using eqn. (8) and imposing the condition that the number of half-wavelengths on the resonant line is kept constant,

$$\frac{\delta\omega}{\omega_0} = \frac{1 - v_0/v_1}{L/l + v_0/v_1 - 1} \quad . . . \quad (9)$$

If the change in phase velocity is small, i.e.  $v_0/v_1 \approx 1$ , the change in resonance frequency is given by

$$\frac{\delta\omega}{\omega_0} = -\frac{l}{L} \left( 1 - \frac{v_1}{v_0} \right) \quad . . . \quad (10)$$

From eqn. (10) it can be seen that, by plotting the change in resonance frequency as a function of the length occupied by the periodic structure, a straight line should be obtained. The phase velocity in the periodic structure will be given by the slope of this line. A decrease in frequency is expected for a wave which is slowed down in the structure.

The experimental procedure was as follows:

The dielectric rod was inserted in the resonator and the oscillator frequency was changed until a resonance was observed;  $\omega_0$  was then measured. The number of half-wavelengths,  $n$ , in the resonator was obtained by moving a thin conducting disc along the rod, with its axis parallel to the rod. The condition for resonance was unaffected only when the obstacle was placed at a node of the electric field. By counting the number of power-transfer maxima on the analyser screen while the obstacle was traversing the length of the resonator, the number of half-wavelengths was found. Copper rods were then added at regular intervals, starting either from the input or output end of the resonator. After each rod had been inserted, the oscillator was again tuned to resonance and the frequency was measured. This procedure was repeated until the whole length of the resonator was occupied by the periodic structure.

The amount of radiation from the structure was indicated by the change in the Q-factor of the resonator, assuming all other losses to be constant. To measure the Q-factor, the oscillator was detuned from resonance on either side until the deflection on the cathode-ray tube was half the value at resonance. The two frequencies thus found corresponded to half-amplitude points of the resonator. The bandwidth was measured either by means of the frequency meter or directly on the screen of the cathode-ray tube with the aid of the 1 Mc/s spaced markers, the first method being more accurate.

### (4) DISCUSSION OF RESULTS

#### (4.1) Determination of Phase Velocities

The diameter  $2a$  of the conducting rods has been kept constant at  $2a = 0.15\text{ cm} \approx 0.015\lambda$ , and the effects of varying the length of rod  $h$  and the spacing  $d$  have been investigated.\* A large number of measurements have been carried out, a typical set being given in Fig. 7. Results are summarized in Figs. 8–10.

In the experiments carried out, a resonance could always be observed in the presence of the periodic structure of conducting rods, and so it was proved that propagation along the structure actually existed. The negative sign of  $\delta f$  indicated that the wave was slowed down along the structure. When the structure was formed by elements of  $h/\lambda > 0.5$ , the Q-factor fell off rapidly as the first elements were inserted and no resonance could be detected. This was expected as the line was then being loaded inductively, which would make  $\lambda_g > \lambda_0$ .

\* The length  $h$  is the effective length of copper rods. The length of the portion of copper rod embedded in the dielectric is multiplied by  $\sqrt{\epsilon_r}$ . Also, since changes of wavelength are small, the normalizing factor  $\lambda$  has been taken as  $\lambda = 10\text{ cm}$  throughout.

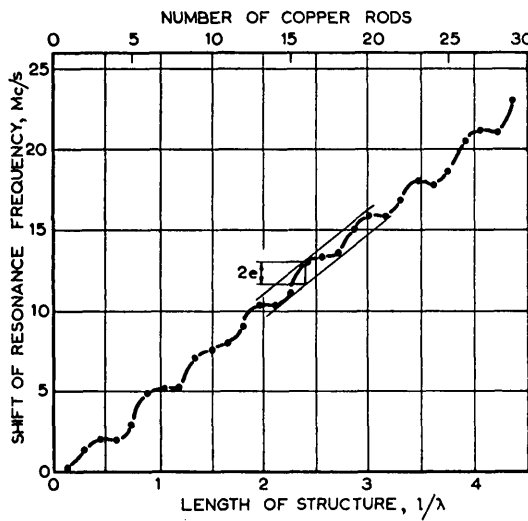


Fig. 7.—Shift of resonance frequency as a function of structure length.  
The rod length is  $0.24\lambda$  and the spacing is  $0.15\lambda$ .

In Fig. 7 the shift in resonance frequency,  $-\delta f$ , is plotted against structure length for closely spaced structures, with  $d/\lambda = 0.15$ . It is seen that the measured values of  $\delta f$  lie on a curve which oscillates with a period of  $\lambda/2$  about a straight line through the origin. From the hypothesis of the existence of a 'slow' wave along the periodic structure and in conjunction with the equivalent circuit of Fig. 6 and eqn. (10), measured values of  $\delta f$  against  $l/L$  are expected to lie on a straight line through the origin, for small reductions in phase velocity. This is, in fact, the case in Fig. 7, apart from the small variations, periodic in  $l$ , superimposed on this line. This oscillation may be explained by the fact that in the equivalent circuit of Fig. 6 the two sections of transmission line have been assumed to be of the same characteristic impedance. This is, however, not the case, since the line has been loaded periodically by capacitive shunt-elements. In the modified equivalent circuit  $Z_0$  and  $Z_1$  are the characteristic impedances of the unloaded and loaded transmission lines, respectively. It is shown in Section 8 that the change in resonance frequency as a function of loaded length  $l$ , for small changes of phase velocity, is given approximately by

$$-\frac{\delta f}{f_0} = t \frac{l}{L} \left(1 - \frac{v_1}{v_0}\right) + (t-1) \frac{\lambda_0}{4\pi L} \sin 4\pi \frac{l}{\lambda_0} \quad . \quad (11)$$

where  $t = Z_1/Z_0$ .

The observed deviations from a straight line in Fig. 7 are evidently explained by eqn. (11). If the maximum vertical deviation is  $2e$ , the absolute value of  $(t-1)$  is given by

$$|t-1| = (2e) 2\pi \frac{L}{\lambda_0} \quad . \quad (12)$$

and for lines with no attenuation  $(t-1)$  is real and either positive or negative. The sign of  $(t-1)$  can be found by observing the phase of the oscillatory deviations in Fig. 7. This is found to be negative, which again is consistent with the fact that  $Z_1$  is the characteristic impedance of a transmission line which has been shunt-loaded capacitively, so that  $Z_1 < Z_0$ .

The treatment leading to eqn. (11) obviously breaks down when the spacing is more than a small fraction of the wavelength. It is now more reasonable to use the equivalent circuit of a transmission line periodically shunt-loaded with reactive elements, shown in Fig. 3. When this analysis is carried out for

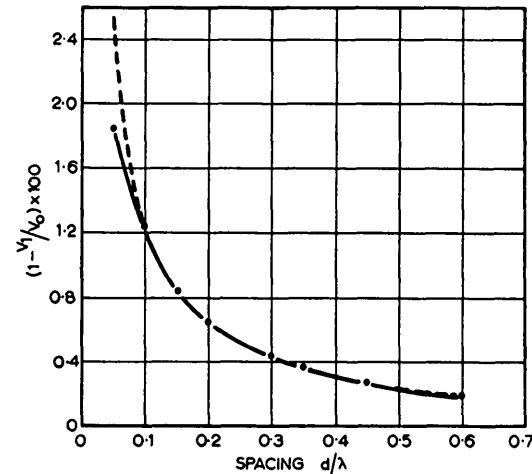


Fig. 8.—Effect of varying the spacing  $d/\lambda$  on the percentage reduction of phase velocity on rod structures.

The rod length is  $0.24\lambda$ .  
The curve of  $(1 - v_1/v_0) = K\lambda/d$  is shown by the broken line, for  $K = 0.125$ .

values of  $d/\lambda$  which are no longer small compared with the wavelength of operation, it is found that the observed deviations from a straight line are adequately explained.

In Fig. 8 the measured change in phase velocity is given as a function of spacing between the conducting rods, for rods of fixed length  $h$ . It is seen that when  $d/\lambda \geq 0.1$  the reduction of phase velocity is given approximately by the simple rule

$$\left(1 - \frac{v_1}{v_0}\right) = K \left(\frac{\lambda}{d}\right) \quad . \quad (13)$$

where  $K$  is a function of  $h$  only.

The experimental results are eventually summarized in Fig. 9, where the change in phase velocity is given as a function of rod length  $h/\lambda$ , with  $d/\lambda$  as parameter.

#### (4.2) Radiation from Yagi Aerials

In the experimental results of the previous Section it had been shown that a surface wave was established in the resonator which propagated along the structure with reduced phase velocity. The fact that a sharp resonance could be observed, even when the rod structure was long in terms of wavelengths, would itself lead to the conclusion that no large amount of power was being radiated from points along the line. However, some more experimental evidence was sought on this point, because it was of some importance to verify the proposition that any radiation from Yagi-type periodic structures occurred not at points along the structure but at the discontinuity at the end of the structure only.<sup>2</sup> A series of experiments was therefore carried out in which the conducting rods were, as in the previously described experiments, inserted in the dielectric guide, but attention was concentrated on the change in the Q-factor of the resonator. It was argued that if radiation occurred from the length of the structure, the Q-factor would decrease continually as  $l/L$ , the length of the loaded section, increased. If, on the other hand, radiation was confined to the discontinuity, the Q-factor should drop initially, then remain constant and finally increase again when  $l/L \rightarrow 1$ , as the discontinuity would then disappear.

Measurements were made on closely-spaced structures of  $d/\lambda = 0.1$  and four different rod lengths  $h/\lambda$ . The absolute values of Q-factor obtained were of the order of several hundred, the main source of losses being the power lost through the

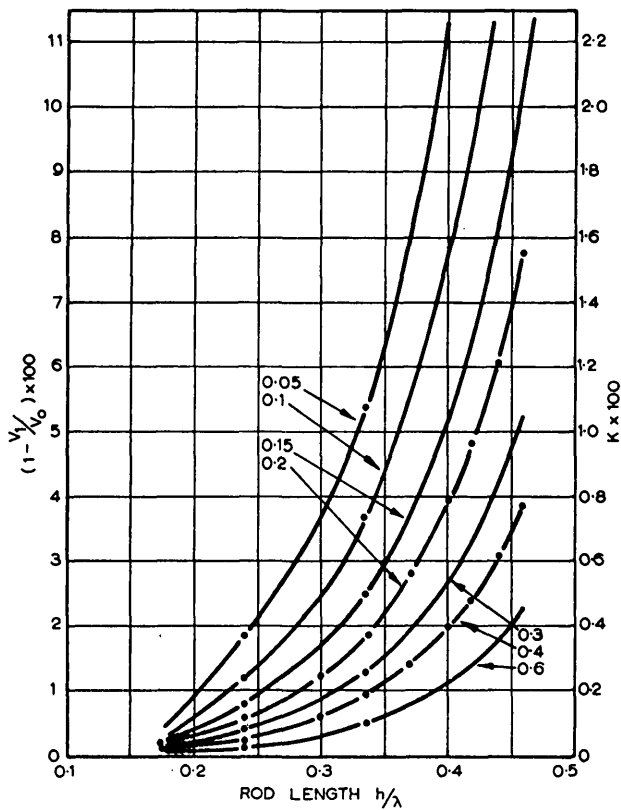


Fig. 9.—Percentage reduction of phase velocity on periodic rod structures.

The parameter is the spacing  $d/\lambda$ .  
The right-hand scale gives the constant  $K$  of eqn. (13).

coupling holes and the effect of finite dimensions of the end-plates, with the result that a small part of the field extended outside the resonator. These effects were of constant magnitude for any particular structure, and the relative Q-factors, i.e. the actually measured Q-factor divided by the initial value when no rods were present, are shown in Fig. 10. It is evident from Fig. 10 that the Q-factor falls from its initial value for the unloaded dielectric rod line to a lower value which depends on the length of the conducting rods. The greater the difference in phase velocity between the periodic structure and the dielectric rod line, the more pronounced is the decrease in the Q-factor. The decreased Q-factor remains almost constant as  $l/L$  is increased, indicating that the amount of loss does not increase. As the periodic structure occupies the whole length  $L$  of the resonator, the Q-factor increases again until, at last, for  $l/L = 1$  it is almost restored to its initial value. Results given in Fig. 10 therefore provide quite conclusive evidence that, unless there is a discontinuity, no radiation takes place from a Yagi-type periodic structure.

It is now suggested that the radiation mechanism of Yagi aerials can be explained in terms of a surface wave propagating along the aerial and a radiating aperture at the end of the aerial structure. By means of a driven element, a surface wave of the dipole-mode type is excited which propagates without radiation along the aerial, and the radiation pattern can be derived from the field distribution in the terminal aperture plane, using eqn. (2). Approximations may now be made on the assumption that the phase-change coefficient,  $\beta$ , of the wave on the structure is almost equal to the free-space phase-change coefficient  $\beta_0$ . Thus, in terms of Cartesian co-ordinates, the field components

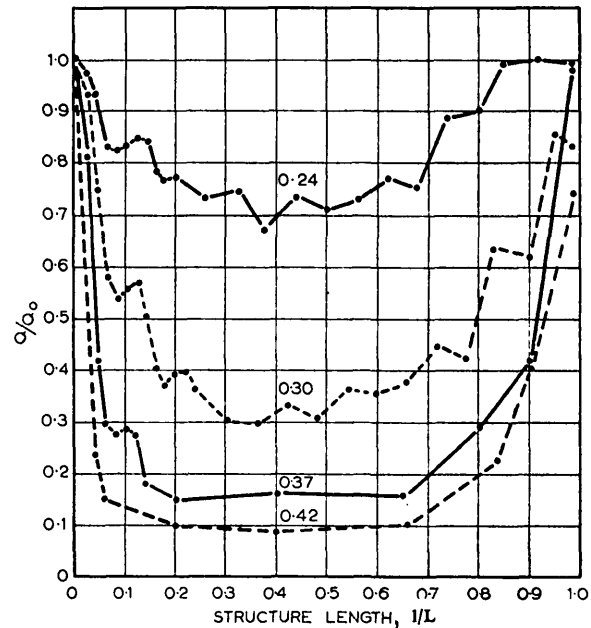


Fig. 10.—Variation of resonator Q-factor with length of rod structure.

The parameter is the rod length  $h/\lambda$ .  
The spacing is kept constant at  $d/\lambda = 0.1$ .  
 $Q_0$  is the value of the Q-factor when no rods are present.

in a transverse plane outside a cylinder  $\rho = h/2$  bounding the rod structure are given by<sup>2</sup>

$$E_x = AK_0(k_0\rho) \quad \dots \dots \dots \quad (14)$$

$$E_y = 0 \quad \dots \dots \dots \quad (15)$$

where  $k_0^2 = \beta^2 - \beta_0^2$  . . . . . (16)

The exact field distribution for  $\rho < h/2$  is not known, but, to the extent of the above-mentioned approximations, the contribution of this part of the radiating aperture can be neglected, since, for  $\lambda_g/\lambda_0 \approx 1$ , a far greater part of the energy of the dipole wave is transmitted outside the structure. Substitution of eqn. (14) into eqn. (2) gives

$$g(\theta, X) = 2\pi A(1 + \cos \theta) \int_{h/2}^{\infty} \rho K_0(k_0\rho) J_0(\beta_0\rho \sin \theta) d\rho \quad (17)$$

which shows that the radiation pattern is independent of  $X$ . This is consistent with observed radiation patterns of long Yagi aerials, which are very similar in the plane of polarization and perpendicular to it.<sup>10</sup>

The integral of eqn. (17) is of the Lommel type, and integration yields

$$g(\theta) = \frac{1}{2}\pi Ah^2(1 + \cos \theta) \frac{\frac{k_0h}{2} K_1\left(\frac{k_0h}{2}\right) J_0(u) - u K_0\left(\frac{k_0h}{2}\right) J_1(u)}{\left(\frac{k_0^2 h^2}{4} + u^2\right)} \quad (18)$$

where  $u = \beta_0 \frac{h}{2} \sin \theta$  . . . . . (19)

The expression in eqn. (18) can be readily evaluated with the help of Tables. This can be carried out for any given reduction in phase velocity, and the resulting half-amplitude beam width is shown in Fig. 11. From this figure and the phase velocities

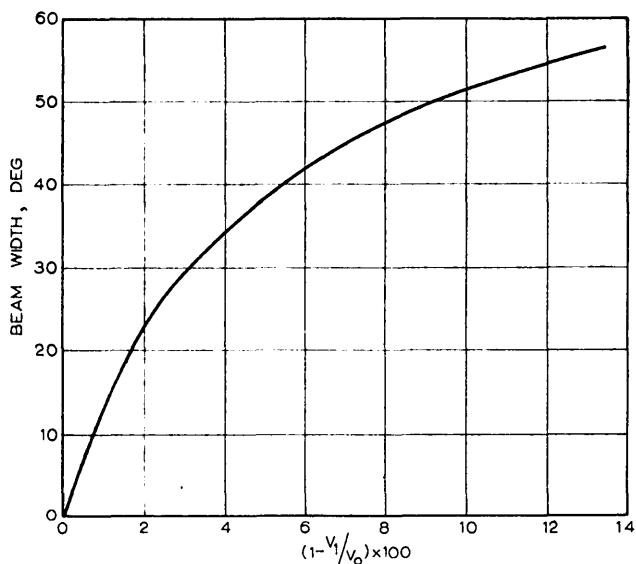


Fig. 11.—Theoretical dependence of half-amplitude beam width on the percentage difference between free-space and dipole-wave phase-velocity.

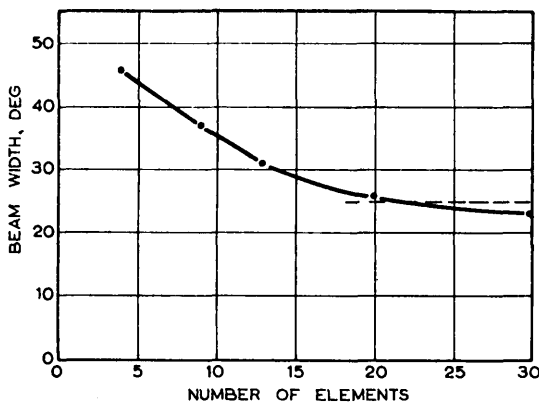


Fig. 12.—Experimental beam width of Yagi aerials from Reference 11.  
The rod length is  $0.4\lambda$  and the spacing is  $0.34\lambda$ .  
The beam width of long Yagi aerials calculated by the method outlined in the paper is shown by the broken line.

obtained from the resonator experiments, the beam width of a long Yagi array can be predicted.

A set of experimental results for long Yagi aerials is shown in Fig. 12, where the aerial length is increased and all other parameters are kept constant.<sup>11</sup> The beam width calculated by the new approach is also indicated. It appears to tend to about 22° for large numbers of director elements. The corresponding theoretical figure, as predicted from Fig. 11, using the experimentally determined dipole-mode wavelength for a structure having the same rod lengths and spacings as the Yagi array, is 25°. Agreement is quite good, although one would expect the theoretical beam width to be smaller than the experimental.

It should be noted, however, that this analysis is strictly valid only when all the power fed to the aerial is converted into a surface wave, and will apply only to aerials which are long in terms of wavelengths. In practice, Yagi aerials are quite short, and some part of the input power is radiated directly from the driven element. The direct radiation from the driven element may either increase or decrease the beam width.<sup>2</sup> The superposition of the two radiation patterns will contribute to the side-lobe structure.

An aerial with short elements would have a larger radiating aperture, as the field of the surface wave becomes more widespread about the guiding structure, resulting in a sharper beam, but at the same time one would expect a lower launching efficiency of the surface wave,<sup>12</sup> resulting in a greater amount of power being radiated directly from the driven dipole, which has a low directivity. The optimum construction of the aerial for best overall performance would have to be found experimentally.

### (5) CONCLUSIONS

It has been shown that a non-radiating plane surface wave is supported by a Yagi-type periodic structure of conducting rods, and that radiation from the structure occurs only from a discontinuity. The rod structure has been found to be analogous to a capacitively loaded transmission line for rod lengths less than  $\lambda/2$ . The dipole wave has been excited on the structure, and in a series of resonator experiments the propagation coefficients have been experimentally determined for structures of different dimensions. With the aid of the aperture field approach the beam width can be predicted when these structures are used as aerials. Results are found to be in good agreement with experimentally observed radiation patterns for long Yagi aerials.

### (6) ACKNOWLEDGMENTS

The work described in the paper was carried out at the Electrical Engineering Department of the Imperial College of Science and Technology, and the author is indebted to Dr. Willis Jackson for the facilities provided. Many thanks are due to Dr. J. Brown for helpful discussions of the problem. The author wishes to acknowledge the award of a British Council Scholarship and a grant from the Technion Society of Great Britain.

### (7) REFERENCES

- (1) PIDDICK, F. B.: 'Currents in Aerials and High Frequency Networks' (Oxford University Press, 1949).
- (2) BROWN, J., and SPECTOR, J. O.: 'The Radiating Properties of End-Fire Aerials', *Proceedings I.E.E.*, Paper No. 2216 R, January, 1957 (104 B, p. 27).
- (3) BARLOW, H. M., and CULLEN, A. L.: 'Surface Waves', *ibid.*, Paper No. 1482 R, April, 1953 (100, Part III, p. 329).
- (4) BROWN, J.: 'The Types of Wave which may exist near a Guiding Surface', *ibid.*, Paper No. 1567 R, November, 1953 (100, Part III, p. 363).
- (5) STRATTON, J. A.: 'Electromagnetic Theory' (McGraw-Hill, 1941).
- (6) SILVER, S.: 'Microwave Antenna Theory and Design' (McGraw-Hill, 1949).
- (7) BARLOW, H. M., and KARBOWIAK, A. E.: 'An Investigation of the Characteristics of Cylindrical Surface Waves', *Proceedings I.E.E.*, Paper No. 1462 R, April, 1953 (100, Part III, p. 321).
- (8) CHANDLER, C. H.: 'An Investigation of Dielectric Rod as Waveguide', *Journal of Applied Physics*, 1949, 20, p. 1188.
- (9) SCHELKUNOFF, S. A.: 'Electromagnetic Waves' (Van Nostrand, 1943).
- (10) ALRED, R. V.: 'Experiments with Yagi Aerials at 600 Mc/s', *Journal I.E.E.*, 1946, 93, Part IIIA, p. 1490.
- (11) FISHENDEN, R. M., and WIBLIN, E. R.: 'Design of Yagi Aerials', *Proceedings I.E.E.*, Paper No. 731 R, January, 1949 (96, Part III, p. 5).
- (12) CULLEN, A. L.: 'The Excitation of Plane Surface Waves', *ibid.*, Monograph No. 93 R, February, 1954 (101, Part IV, p. 225).

## (8) APPENDIX: The Resonant Frequency of a Two-Section Transmission Line Short-Circuited at Both Ends

Let  $Z_0$  and  $Z_1$  be the characteristic impedances of the two sections of short-circuited transmission line shown in Fig. 6. The condition for resonance at a frequency  $\omega$  is given by

$$Z_0 \tan \frac{\omega}{v_0} (L - l) + Z_1 \tan \frac{\omega}{v_1} l = 0 \quad . . . \quad (20)$$

where  $v_1$  is the phase velocity on the section of impedance  $Z_1$  and length  $l$ , and  $v_0$  is the phase velocity on the section of impedance  $Z_0$  and length  $(L - l)$ . For a small change in resonance frequency we have

$$\omega = \omega_0 + \delta\omega \quad . . . \quad (21)$$

where the frequency of resonance for  $l = 0$  is denoted by  $\omega_0$  and is given by  $\omega_0/v_0 L = n\pi$ . If now the value of  $\delta\omega/\omega$  is made sufficiently small, substitution of eqn. (21) into eqn. (20) yields

$$\begin{aligned} \frac{\delta\omega}{v_0} (L - l) \sec^2 \frac{\omega_0 l}{v_0} - \tan \frac{\omega_0 l}{v_0} \\ + t \left( \frac{\delta\omega}{v_1} l \sec^2 \frac{\omega_0 l}{v_1} + \tan \frac{\omega_0 l}{v_1} \right) = 0 \quad (22) \end{aligned}$$

where  $t = Z_1/Z_0$ . Let it be assumed that the phase velocities of the two sections differ by a small amount only,

$$v_1 = v_0 + \delta v \quad . . . \quad (23)$$

Substituting eqn. (23) into eqn. (22) and neglecting second-order infinitesimals, we have

$$-\frac{\delta\omega}{\omega_0} = \frac{tl \left( 1 - \frac{v_1}{v_0} \right) + \frac{v_0}{\omega_0} \left( \frac{t-1}{2} \right) \sin 2 \frac{\omega_0 l}{v_0}}{L \left[ 1 - \frac{l}{L} \left( 1 - \frac{v_0}{v_1} t \right) \right]} \quad . \quad (24)$$

Assuming the value of the impedance ratio  $t$  to be near unity, and also writing

$$\frac{\omega_0}{v_0} = \frac{2\pi}{\lambda_0}$$

we have

$$-\frac{\delta\omega}{\omega_0} = t \frac{l}{L} \left( 1 - \frac{v_1}{v_0} \right) + (t-1) \frac{\lambda_0}{4\pi L} \sin 4\pi \frac{l}{\lambda_0} \quad . \quad (25)$$

which becomes identical with eqn. (10) on making  $t = 1$ .